Nematic liquid-crystal director configuration for general elastic coefficients

Elsebeth Schröder*
Department of Applied Physics, Chalmers University of Technology and Göteborg University, S-41296 Gothenburg, Sweden
(Received 4 May 2000)

We provide a general analytical solution for the director field of a nematic liquid crystal confined between two horizontal plates. The derivation goes beyond the common one-constant approximation where the elastic coefficients are assumed equal. The solution remains valid in the presence of an applied magnetic or electric field. The effect on the bulk director of various director anchoring angles at the confining plates is derived and analyzed. Further, a generalization of the Freedericksz transition to other anchoring angles is investigated.

PACS number(s): 61.30.Gd, 61.30.Cz, 64.70.Md, 78.20.−e

The nematic liquid crystal (NLC) state of matter is the simplest state with an anisotropic electromagnetic response. The elongated molecules of the NLC have random positions but align themselves along an average direction, thus providing the liquid with directional order and positional isotropy [1,2]. Various biological molecules and membranes, surfactants, and emulsifiers are important examples of materials with liquid-crystal states [3], and there is extensive technological use of synthesized liquid crystals for optical displays. It is of significant importance to provide a mesoscopic link between the microscopic and macroscopic descriptions of materials in a simple model.

Obtaining an analytical description of, for example, the NLC configuration as a function of anchoring conditions strengthens this mesoscopic link. First-principles atomic-scale accounts of the molecule-surface interaction, the anchoring, can then directly be related to the macroscopic, measurable, NLC behavior. One can thus experimentally verify microscopic calculations of the parameters in the mesoscopic model or, conversely, use the macroscopic phenomena, e.g., optical response, to characterize microscopic surface structure.

Here we provide such an analytical description for a NLC subject to an applied magnetic or electric field and evaluate, in particular, the optical response as a function of anchoring conditions. We consider a slab of the NLC confined between two planar plates, the simplest model system that is both characteristic for a key liquid-crystal situation and yet available for experimental study. The theoretical approaches to the system so far either (a) use a simplifying assumption (the ''one-constant approximation'') on the elastic properties of the NLC, (b) do not allow for an applied electric or magnetic field, (c) consider only cases where the molecules at the plates are parallel and/or perpendicular to the plates, or (d) deal with the system numerically or using approximations [4,5].

The present approach permits a discussion of the NLC behavior as a function of the material constants and the molecular directions at the boundaries (anchoring angles). The paper shows that a detailed theoretical description beyond the numerical approach can be obtained without such simplifying assumptions. For the model system of a NLC between two plates a general analytical solution is derived in terms of Legendre third elliptic functions for the variation in average molecular direction within the NLC. In this way important insights into the operating mechanism behind several NLC applications are provided, such as a generalization of the Freedericksz transition and the characterization of surfaces using NLC films or droplets [5,6].

The analytical solution of the NLC molecular directions has several important implications. (I) It is given in terms of established special functions, the third elliptic integrals, for which well-documented numerical routines exist [7]. (II) Most importantly, with an analytical solution available, the NLC system can be efficiently and extensively analyzed, allowing identification, characterization, and understanding of the dependence of important NLC system behavior on material and system parameters. This is exemplified here by the results for the dependence of the optical transmission on parameters like the strength of the applied field, the elastic coefficients, and the anchoring angles.

In the following, the model system is presented and the equations describing the NLC are identified and solved. We emphasize that the solutions are analytic and that they are valid for general anchoring conditions, as long as the anchoring does not create twist in the NLC. The ''traditional'' planar Freedericksz transition (PFT) is a second-order phase transition breaking the homogeneous molecular order in a cell with parallel planar anchoring [1] at sufficiently strong applied fields. We investigate a generalization of the PFT to a system with general anchoring angles and we find the values of the applied fields at which this transition takes place. The transition for parallel but nonplanar anchoring has been treated previously [5]. Further, we use the solution to describe also nematic wetting films and droplets that are used to characterize the structure of the surface they wet.

Macroscopically, the NLC may be described by a continuous vector field $\boldsymbol{n}(\boldsymbol{r})$, a director field, representing the local average direction of the molecules at position $\boldsymbol{r}$. For symmetry reasons a NLC between extended parallel plates is translationally invariant in the plane of the plates, and in our model the director field can be written as $\boldsymbol{n}(z) = (\sin\theta(z), 0, \cos\theta(z))$ where θ is the angle between the director and the z axis (Fig. 1). The inset of Fig. 1(a) illustrates the director field between the plates.

We assume that the (magnetic or electric) field applied vertically to the NLC can be considered uniform across the

*Email address: schroder@fy.chalmers.se

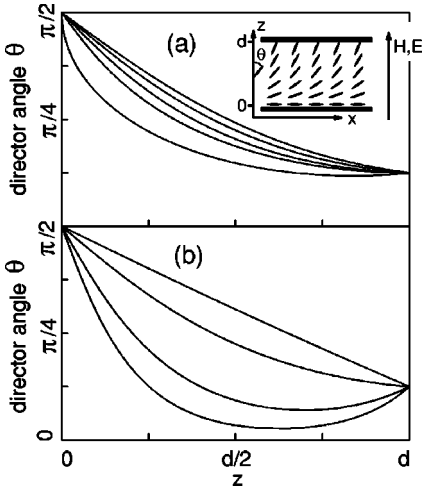

FIG. 1. The NLC director field. (a) The director angle θ versus the vertical position z. At fixed $m=2$ the elastic anisotropy runs through $\kappa=0$, 0.25, 0.5, 0.75, 1 (top to bottom curves) with anchoring angles $\theta_b=\pi/2$ and $\theta_t=\pi/8$. Inset: Illustration of the two horizontal plates enclosing the NLC, at $m=2$ and $\kappa=0.25$. The director field is represented by the small sticks. (b) Director angle $\theta(z)$ at fixed $\kappa=0.25$ for applied fields $m=0$ (top curve), 2, 4, 6 (bottom curve).

sample. The assumption is reasonable as long as the anisotropy of the NLC is small. This is the case for the diamagnetic anisotropy $\mu_a=\mu_{||}-\mu_\perp$, defined as the difference between the magnetic permeabilities parallel and perpendicular to the director, and in some NLCs for the dielectric anisotropy $\varepsilon_a=\varepsilon_{||}-\varepsilon_\perp$ [8]. The diamagnetic anisotropy μ_a is always positive, and for applied electric fields we assume that the NLC also has positive ε_a. Systems with $\varepsilon_a<0$ can be dealt with analogously.

In typical realizations the surfaces of the plates have been treated [9] such that the molecules align uniformly in one direction at the top plate and uniformly in a different direction at the bottom plate. We assume that the director cannot deviate from these directions at the plates, no matter how strong the applied field is (strong anchoring). Moreover, we retain one restriction from the PFT, namely, that the entire director field, including the top and bottom anchoring, is contained within a vertical plane [the x-z plane, inset in Fig. 1(a)]. In other words, twist is not considered. We denote the anchoring angles by $\theta(z=0)=\theta_b$ and $\theta(z=d)=\theta_t$.

We proceed by identifying the Helmholtz free energy and the Euler-Lagrange equations in a standard way [1]. The elastic part of the free energy is, to lowest order in $\nabla \boldsymbol{n}$, given by the Frank-Oseen-Zocher [10] description

$$f_d=\frac{K_1}{2}(\nabla\cdot\boldsymbol{n})^2+\frac{K_2}{2}(\boldsymbol{n}\cdot\nabla\times\boldsymbol{n})^2+\frac{K_3}{2}[\boldsymbol{n}\times(\nabla\times\boldsymbol{n})]^2,$$

where K_1, K_2, and K_3 are the bulk splay, twist, and bend elastic coefficients of the NLC.

When an external field is applied to the sample the free energy density receives a contribution of [11,12]

$$f_a=\begin{cases}-\frac{1}{2}\mu_0\{\mu_\perp H^2+\mu_a(\boldsymbol{n}\cdot\boldsymbol{H})^2\} & \text{(magnetic)}\\ -\frac{1}{2}\varepsilon_0\{\varepsilon_\perp E^2+\varepsilon_a(\boldsymbol{n}\cdot\boldsymbol{E})^2\} & \text{(electric)}.\end{cases}$$

From the total free energy density f_d+f_a the Euler-Lagrange equation for vertically applied fields may be obtained:

$$\frac{\sin 2\theta}{2}\left\{\kappa\left(\frac{\partial\theta}{\partial\xi}\right)^2+\alpha^2m^2\right\}-(1-\kappa\sin^2\theta)\frac{\partial^2\theta}{\partial\xi^2}=0. \quad (1)$$

Here m was introduced as the reduced magnetic potential $m=(\mu_a\mu_0/K_3)^{1/2}Hd$ and the reduced voltage $m=(\varepsilon_a\varepsilon_0/K_3)^{1/2}Ed$, respectively, depending on the type of field applied. The ratio $\kappa=(K_3-K_1)/K_3$ is the anisotropy of the elastic coefficients. Typically $K_3>K_1$ and thus $0\leqslant\kappa<1$. Furthermore, the spatial coordinates were rescaled to $\xi=z/(\alpha d)$ where d is the separation of the plates, and initially we assume $\alpha=1$.

At this point, a few comments on the limitations for our analytical solution are appropriate. One restriction has already been mentioned, namely, that (i) the director at the top and bottom plates must be in the same vertical plane. This is immediately fulfilled if one of the anchoring directions, say the top anchoring, is vertical ($\theta_t=0$). In addition, (ii) the director angle θ is restricted to the interval $[0,\pi/2]$. Also, we will at first make use of the restriction that (iii) $\theta(z)$ is strictly monotonic throughout the system, except at the boundaries where $\partial\theta/\partial z$ is allowed to be zero. This condition is broken if the applied field exceeds a critical value $m_{\rm crit}$. The bulk then becomes more aligned with the applied field than θ_b and θ_t. For $\theta_b=\theta_t=\pi/2$ this is the PFT. Below we show how rescaling ($\alpha<1$) overcomes restriction (iii).

As a result of the monotony requirement (iii), Eq. (1) can be integrated once to yield

$$c+\alpha^2m^2\sin^2\theta=(1-\kappa\sin^2\theta)\left(\frac{\partial\theta}{\partial\xi}\right)^2 \quad (2)$$

or, equivalently,

$$\xi=\mathrm{sgn}(\theta_t-\theta_b)\int_{\theta_b}^{\theta}\sqrt{\frac{1-\kappa\sin^2\theta}{c+\alpha^2m^2\sin^2\theta}}\,d\theta. \quad (3)$$

The integration constant c is determined from the top boundary condition. The second requirement, that $0\leqslant\theta\leqslant\pi/2$, permits a change of integration variable $h(\theta)=\arcsin\{\cos\theta(1-\kappa\sin^2\theta)^{-1/2}\}$. After some algebra the inverse solution to the differential equation (1) is obtained as a simple ratio of third elliptic integrals [13],

$$\xi(\theta)=\frac{z(\theta)}{\alpha d}=\frac{\Pi(\kappa,h(\theta),\eta)-\Pi(\kappa,h(\theta_b),\eta)}{\Pi(\kappa,h(\theta_t),\eta)-\Pi(\kappa,h(\theta_b),\eta)}. \quad (4)$$

Here we have introduced $\eta=(c\kappa+\alpha^2m^2)/(c+\alpha^2m^2)$ where the integration constant c is given by

$$c+\alpha^2m^2=(1-\kappa)^2\{\Pi(\kappa,h(\theta_t),\eta)-\Pi(\kappa,h(\theta_b),\eta)\}^2. \quad (5)$$

Equations (4) and (5) constitute our result for a constant, uniform magnetic (electric) field through a material with a positive diamagnetic (dielectric) anisotropy, at applied voltage or magnetic potential $m<m_{\rm crit}$ and anchoring angles θ_b and θ_t.

Figure 1 illustrates the variation of the director field with changing κ and applied field. As an example, we plotted the director angle $\theta(z)$ for $\theta_t=\pi/8$ and $\theta_b=\pi/2$. In Fig. 1(a) we fix the applied field and change the elastic coefficients. When the splay elastic coefficient K_1 is considerably smaller than the bend elastic coefficient K_3 (i.e., $\kappa\simeq 1$) the energy cost of splay compared to bend is low. The system therefore tends to favor a configuration in which the molecules turn within a narrow region. This is evident in Fig. 1(a) for $\kappa=1$.

In Fig. 1(b) we fixed the elastic coefficients at $\kappa=0.25$, plotting $\theta(z)$ for various strengths of the applied field m. We see that at a value of m between 2 and 4 the director field is no longer monotonic; we return to this below.

Figure 1 covers the relevant field strengths for magnetic as well as electric fields. In a typical realization the parameters are $\mu_a\approx 4\pi\times 10^{-7}$, $d\approx 20$ μm, and $K_3\approx 10^{-11}$ N. The value $m=6$ thus roughly corresponds to $H\approx 8\times 10^5$ A/m or $B\approx\mu_0 H\approx 0.9$ T. Replacing μ_a by $\varepsilon_a\approx 0.1$ yields an electric field of $E\approx 10^6$ V/m, or an applied voltage across the sample of 20 V.

The solution of the director field given by Eqs. (4) and (5) for $\alpha=1$ is valid when the applied field is subcritical, $m<m_{\rm crit}$. We now turn to look at the director configuration in stronger fields, $m\geqslant m_{\rm crit}$. In this case the director angle has its minimum value $\theta^*=\theta(\alpha d)$ at a vertical position αd between the plates, $0<\alpha\leqslant 1$. The position αd and the angle θ^* clearly depend on the strength of the applied field.

For $m\geqslant m_{\rm crit}$ the NLC can be described as two adjoining slabs each with a monotonic director field. The Euler-Lagrange equation (1) is valid in each slab, with the boundary conditions θ_b and θ^*, or θ^* and θ_t, respectively. Because $\partial\theta/\partial z=0$ at θ^* the integration constant is now found directly as $c=-\alpha^2 m^2\sin^2\theta^*$, and the director field in both slabs is given by Eq. (4) when η is replaced by $\eta^*=(1-\kappa\sin^2\theta^*)/\cos^2\theta^*$ and the appropriate anchoring conditions are used. Further, the position αd and the director angle θ^* of the slab interface are found as the inverse solutions of

$$m=\frac{1-\kappa}{\cos\theta^*}\{2\Pi(\kappa,h(\theta^*),\eta^*)-\Pi(\kappa,h(\theta_b),\eta^*)-\Pi(\kappa,h(\theta_t),\eta^*)\},\tag{6}$$

$$\frac{1-\alpha}{\alpha}=\frac{\Pi(\kappa,h(\theta^*),\eta^*)-\Pi(\kappa,h(\theta_t),\eta^*)}{\Pi(\kappa,h(\theta^*),\eta^*)-\Pi(\kappa,h(\theta_b),\eta^*)}.\tag{7}$$

This includes the PFT for which the smallest director angle θ^* is given by $m=2(1-\kappa)\Pi(\kappa,h(\theta^*),\eta^*)/\cos\theta^*$.

The relation (6) is illustrated in Fig. 2(a). For parallel anchoring we see the expected smoothing of the second-order PFT as $\theta_t=\theta_b$ deviates from $\pi/2$. For nonparallel anchoring $\theta^*(m)$ has a more complicated behavior. Without loss of generality we can assume that $\theta_b>\theta_t$. We then find from Eq. (6) that the onset of nonmonotony of the director is at

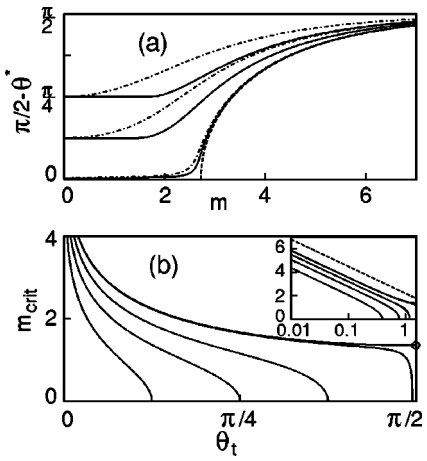

FIG. 2. (a) The minimum angle θ^* as a function of the applied field m. The panel includes the traditional second-order Freedericksz transition of $\theta_b=\theta_t=\pi/2$ (− − −), the transition for parallel anchoring $\theta_b=\theta_t=\pi/4$, $3\pi/8$, $0.99\pi/2$ (− · − · −), and nonparallel anchoring $\theta_b=\pi/2$, $\theta_t=\pi/4$, $3\pi/8$, $0.99\pi/2$ (——). (b) The critical value $m_{\rm crit}$ of the applied field as a function of the top anchoring angle θ_t for various bottom anchoring angles $\theta_b=\pi/8$, $\pi/4$, $3\pi/8$, $0.99\pi/2$, $\pi/2$, from left to right, at $\kappa=0.25$. Inset: Semilogarithmic plot of $m_{\rm crit}$ (——) and $-\ln\theta_t+$const (− − −).

$$m_{\rm crit}=\frac{1-\kappa}{\cos\theta_t}\{\Pi(\kappa,h(\theta_t),\eta_t)-\Pi(\kappa,h(\theta_b),\eta_t)\},\tag{8}$$

here with $\eta_t=(1-\kappa\sin^2\theta_t)/\cos^2\theta_t$. We also find, as expected, that parallel anchoring simply has $m_{\rm crit}=0$ except at the PFT where $m_{\rm crit}=\pi(1-\kappa)^{1/2}$ [1].

In Fig. 2(b) we illustrate how this critical field strength strongly depends on the two anchoring angles. We show the critical field as a function of the top anchoring angle for bottom anchoring angles in the range $\pi/8\leqslant\theta_b\leqslant\pi/2$. The figure demonstrates that, except for a few special situations, the configuration remains monotonic for small applied fields. As the top anchoring gets closer to vertical, the field needed for the monotony to break down diverges logarithmically,

$$m_{\rm crit}=-\ln\theta_t+f(\theta_b,\kappa)+O(\theta_t),\tag{9}$$

as illustrated in the inset of Fig. 2(b). Thus, if one of the plates has homeotropic anchoring the director field will be monotonic in any applied field m.

We next illustrate the use of the solutions found here to determine the intensity of polarized light transmitted through a NLC film or droplet. The intensity strongly depends on the orientation of the director within the NLC, and since the anchoring angles influence the bulk orientation, measurements of light transmission can be used to characterize the surface on which the NLC rests. In Figs. 3(a)–3(c) the bottom surface is an inhomogeneous material that imposes different bottom anchoring in each of the domains shown. Accordingly, measuring the transmitted intensity of each domain for various external conditions (changes in applied field, turned polarization, changes in wavelength of light, etc.) the anchoring angles, and thus information on the surface structure, can be inferred by inverse methods.

Figure 3(d) shows a calculation of the intensity through a droplet on a surface, using the solution (4) and neglecting

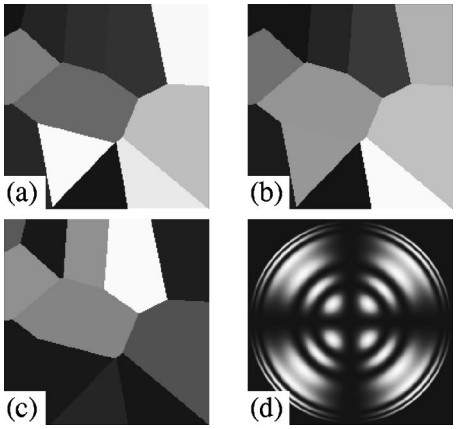

FIG. 3. Intensity of polarized light (wavelength 633 μm) transmitted through (a)–(c) a 20 μm thick NLC film on top of an inhomogeneous substrate or (d) a wetting droplet. (a) No applied field. (b) Applied field $m=1$. (c) Polarization turned $\pi/4$ with respect to (a). (d) Droplet on a self-assembled monolayer (SAM) of organic molecules. The anchoring is homeotropic ($\theta_b=0$) at the SAM-NLC interface and normal to the surface at the NLC-air interface.

radial dependence of the NLC. Gupta and Abbott [6] proposed that droplets of NLC may be used for *in situ* characterization of organic surfaces, and they measured experimentally and derived by numerical simulations transmitted light intensities through 4-*n*-pentyl-4′-cyanobiphenyl (5CB) droplets. In Fig. 3(d) we use the material parameters relevant for the 5CB droplet: $\kappa\approx 0.25$ ($\kappa=0$ was used in [6]), ordinary and extraordinary refractive indices $n_o=1.5$, $n_e=1.7$, wetting angle 57°, and radius at base 250μm. The intensity profile agrees very well with the experiments and simulations of Ref. [6].

In conclusion, with Eqs. (4) and (5) we provided an analytical expression for the director angle of a NLC confined between parallel plates, with general nontwist anchoring conditions, any values of the splay and bend elastic coefficients $K_1 \leqslant K_3$, and an external field applied normal to the plates. Such an analytical solution as a function of material and system parameters will in the future be important for linking atomic-scale properties at the plate interface to macroscopic bulk behavior, thereby bridging the gap between micro- and macroscales. We furthermore used the director configuration found in Eqs. (4) and (5) to calculate the intensity profile of a NLC film and droplet as a probe of the NLC-plate interface structure, and compared the droplet data to experiments and numerical simulations. In Eq. (8) we found the critical applied field below which the director configuration $\theta(z)$ is monotonic. This is a generalization of the planar Freedericksz transition to anchoring angles that are away from planar and not necessarily equal at the top and bottom plates.

The author thanks L. Kramer for stimulating discussions and P. Hyldgaard for critical readings and comments. The author gratefully acknowledges financial support from EU Grant No. ERBFMRXCT960085 and the Materials Consortium No. 9—supported by the Swedish Foundation for Strategic Research (SSF).

[1] See, e.g., P.-G. de Gennes, *The Physics of Liquid Crystals* (Clarendon Press, Oxford, 1974).

[2] M. Kléman, *Points, Lines and Walls in Liquid Crystals, Magnetic Systems and Various Ordered Media* (John Wiley & Sons, Chichester, 1983).

[3] J.W. Goodby, Liq. Cryst. **24**, 25 (1998).

[4] H.J. Deuling, in *Liquid Crystals*, edited by L. Liebert, Solid State Physics Suppl. 14 (Academic, New York, 1978), p. 77; U.D. Kini, J. Phys. II **5**, 1841 (1995).

[5] L.G. Fel and G.É. Lasene, Kristallografiya **31**, 726 (1986) [Sov. Phys. Crystallogr. **31**, 428 (1986)].

[6] V.K. Gupta and N.L. Abbott, Langmuir **15**, 7213 (1999).

[7] See, e.g., W.H. Press, S.A. Teukolsky, W.T. Vetterling, and B.P. Flannery, *Numerical Recipes*, 2nd ed. (Cambridge University Press, Cambridge, 1994).

[8] Examples of NLCs with small dielectric anisotropies ε_a are presented by W.H. de Jeu, in Ref. [4], p. 109, and references therein.

[9] M. Monkade, M. Boix, and G. Durand, Europhys. Lett. **5**, 697 (1988); B. Jérôme, Rep. Prog. Phys. **54**, 391 (1991); A. Gharbi, F.R. Fekih, and D. Durand, Liq. Cryst. **12**, 515 (1992).

[10] C.W. Oseen, Trans. Faraday Soc. **29**, 883 (1933); H. Zocher, *ibid.* **29**, 945 (1933); F.C. Frank, Discuss. Faraday Soc. **25**, 19 (1958).

[11] Throughout this Brief Report metric units are used.

[12] L.D. Landau, E.M. Lifshitz, and L.P. Pitaevskiĭ, *Electrodynamics of Continuous Media*, 2nd ed. (Butterworth-Heinemann Ltd., Oxford, 1995).

[13] The notation used in this Brief Report for the Legendre elliptic integral of the third kind is $\Pi(b,\theta,a^2)=\int_0^\theta (1-b\sin^2\varphi)^{-1}(1-a^2\sin^2\varphi)^{-1/2}d\varphi$.